AGU PUBLICATIONS

Geophysical Research Letters

RESEARCH LETTER
10.1002/2016GL069835

Key Points:
- The Southern Hemisphere circulation response to volcanic forcing is a robust positive annular mode
- Models and observations are not contradictory, as internal variability is large
- ENSO state can explain the perceived discrepancy between observations and models

Supporting Information:
- Supporting Information S1

Correspondence to:
M. C. McGraw,
mmcgraw@atmos.colostate.edu

Citation:
McGraw, M. C., E. A. Barnes, and C. Deser (2016), Reconciling the observed and modeled Southern Hemisphere circulation response to volcanic eruptions, *Geophys. Res. Lett.*, *43*, doi:10.1002/2016GL069835.

Received 31 MAY 2016
Accepted 23 JUN 2016
Accepted article online 27 JUN 2016

Reconciling the observed and modeled Southern Hemisphere circulation response to volcanic eruptions

Marie C. McGraw[1], Elizabeth A. Barnes[1], and Clara Deser[2]

[1]Department of Atmospheric Science, Colorado State University, Fort Collins, Colorado, USA, [2]Climate and Global Dynamics Division, National Center for Atmospheric Research, Boulder, Colorado, USA

Abstract Confusion exists regarding the tropospheric circulation response to volcanic eruptions, with models and observations seeming to disagree on the sign of the response. The forced Southern Hemisphere circulation response to the eruptions of Pinatubo and El Chichón is shown to be a robust positive annular mode, using over 200 ensemble members from 38 climate models. It is demonstrated that the models and observations are not at odds, but rather, internal climate variability is large and can overwhelm the forced response. It is further argued that the state of the El Niño–Southern Oscillation can at least partially explain the sign of the observed anomalies and may account for the perceived discrepancy between model and observational studies. The eruptions of both El Chichón and Pinatubo occurred during El Niño events, and it is demonstrated that the Southern Annular Mode anomalies following volcanic eruptions are weaker during El Niño events compared to La Niña events.

1. Introduction

Volcanic eruptions constitute a large source of natural climate variability on interannual timescales and exert a substantial influence on global climate [e.g., *Santer et al.*, 2013; *Robock*, 2000, and references therein]. The sulfuric acid particles that form in the aftermath of a volcanic eruption reflect incoming solar radiation and absorb terrestrial longwave radiation, leading to a warming in the lower stratosphere and cooling in the troposphere that is often considered the signature of volcanic influence on climate [*Robock*, 2000]. Tropical eruptions exert a greater influence on global climate compared to higher-latitude eruptions [e.g., *Robock and Mao*, 1995; *Robock*, 2000], as their sulfuric acid particles are most efficiently distributed throughout the stratosphere via the stratospheric overturning circulation [e.g., *Trepte et al.*, 1993; *Hitchman et al.*, 1994] and as the transport of volcanic aerosols to the poles acts to enhance the equator-to-pole temperature difference via both radiative effects and effects on ozone chemistry [e.g., *Stenchikov et al.*, 2002; *Solomon*, 1999]. Observations of global climate anomalies in the aftermath of volcanic eruptions are limited, as only two large tropical eruptions have occurred since the beginning of the satellite era in 1979: El Chichón in April 1982 and Pinatubo in June 1991. With such a small sample size, the evaluation of the climate response (particularly that of the tropospheric circulation) to volcanic eruptions has proven difficult, with many studies often finding apparently contradictory results.

Recent research has attempted to reconcile the seemingly conflicting results in models and in observations. Global climate models have been used, with mixed results, to try to isolate a forced response from internal variability. While multiple studies found a Northern Annular Mode (NAM, the primary mode of extratropical variability in the Northern Hemisphere) state similar to observations following eruptions in individual model simulations [e.g., *Graf et al.*, 1993; *Stenchikov et al.*, 2002; *Rozanov et al.*, 2002], other studies [e.g., *Driscoll et al.*, 2012] did not find a significant response in the model simulations performed for the Coupled Model Intercomparison Project, phase 5 (CMIP5) [*Taylor et al.*, 2012]. Positive NAM and North Atlantic Oscillation (NAO) responses have been observed after both tropical and extratropical volcanoes [e.g., *Christiansen*, 2008], suggesting that models and observations are not presenting a consistent picture of the Northern Hemisphere circulation anomalies following volcanic eruptions.

The Southern Hemisphere response is even more muddled. For example, *Roscoe and Haigh* [2007] concluded that eruptions force negative tropospheric Southern Annular Mode (SAM, the primary mode of extratropical variability in the Southern Hemisphere) anomalies based on a multilinear regression of the SAM index against volcanic aerosol loading. *Robock et al.* [2007] found no significant SAM anomalies in reanalysis data sets or in

the NASA GISS-E model following eruptions, attributing what few anomalies they did see in the observations to the concurrent El Niño event. However, *Karpechko et al.* [2010] composited the Southern Hemisphere circulation response to Pinatubo and El Chichón in the CMIP, phase 3 (CMIP3) models and found a positive SAM response in both the stratosphere and the troposphere in spring and fall after the eruptions. The observed SAM was negative following both eruptions, highlighting an apparent disagreement between models and observations. What could be driving these differences?

Volcanic eruptions are thought to impact the tropospheric circulation by strengthening the wintertime stratospheric polar vortex and impacting planetary wave propagation [*Perlwitz and Graf*, 1995]. Some studies [e.g., *Ottera*, 2008; *Stenchikov et al.*, 2006] argue that stratospheric polar vortices in models are generally too strong, which could affect their tropospheric responses to volcanoes. Several studies [e.g., *Karpechko et al.*, 2010; *Barnes et al.*, 2016] suggest that the state of the El Niño–Southern Oscillation (ENSO) could play a role in the perceived discrepancies between modeled and observed SAMs following volcanoes.

Indeed, recent research by *Lehner et al.* [2016] has demonstrated the impact of ENSO state on the global mean surface temperature (GMST) response to volcanic forcing by compositing the modeled and observed GMST responses to three tropical eruptions—Agung, El Chichón, and Pinatubo. While the full suite of CMIP5 models leads to an overestimation of the GMST response when compared to observations, subsampling the models according to whether they happen to simulate a concurrent El Niño event as observed improves the fidelity of the response [*Lehner et al.*, 2016]. *Barnes et al.* [2016] apply a similar technique to the SAM response following Pinatubo, finding that models with positive ENSO states had weak or negative SAM anomalies. However, *Barnes et al.* [2016] looked at only one eruption (Pinatubo) and analyzed only 13 CMIP5 models with a single ensemble member each. Here we use over 200 simulations composited over two eruptions in order to more fully evaluate the Southern Hemisphere circulation response to volcanic forcing as well as the variability of this response and to robustly assess the impact of ENSO in hopes of reconciling the apparent discrepancy between the models and the observations.

2. Data and Methods

2.1. Model Simulations and Reanalysis Data

The primary set of model simulations analyzed here is the 42-member Community Earth System Model (CESM1) Large Ensemble (hereafter CESM-LE) [*Kay et al.*, 2015]. These simulations begin in 1920 and follow the forcing protocol of the CMIP5 models [*Taylor et al.*, 2012]. Each ensemble member has initial atmospheric temperature perturbations on the order of 10^{-14}°C but are otherwise identical, and together, the ensemble members allow for a robust assessment of internal variability. We analyze monthly mean zonal winds at 30 pressure levels, 10 m zonal winds, and surface temperatures over two 25 year climatological base periods centered on two tropical volcanic eruptions—the Pinatubo eruption of June 1991 and the El Chichón eruption of April 1982. We also analyze a 10-member ensemble of CESM1 "Pacemaker" simulations (hereafter CESM-Pacemaker) [*Lehner et al.*, 2016] in the same manner. These simulations use the identical model, forcing, and initial condition protocol as the CESM-LE, but their sea surface temperature (SST) anomalies in the eastern tropical Pacific (20°S–20°N, 180°W to the American coast) are nudged to observations using the NOAA Extended Reconstruction Sea Surface Temperature, version 3 data set (ERSSTv3b), following *Kosaka and Xie* [2013]. In this way, the observed evolution of ENSO is maintained in each simulation, with the rest of the coupled climate system free to evolve. The CESM-LE members, by contrast, have their own internally generated, independent sequences of ENSO events, thus ensuring a wide range of ENSO states following the volcanic eruptions.

To evaluate the observed SAM state following El Chichòn and Pinatubo, we use zonal mean zonal winds, surface temperature, and 10 m zonal winds from the Modern-Era Retrospective Analysis data set (MERRA) [*Rienecker et al.*, 2011]. Finally, 155 simulations from 37 different models in the CMIP5 Historical simulations are compared to the CESM-LE in order to test the results across a full suite of models. Some CMIP5 models do not have strong enough stratospheric temperature responses to volcanic forcing and were thus eliminated from this analysis [see also *Santer et al.*, 2013]; a detailed description of this evaluation can be found in the supporting information. Significance is assessed using a one-sided signed rank test at 95% confidence unless otherwise noted; we use the one-sided test as we hypothesize a priori that the SAM response to volcanic forcing will be positive based on the results of *Karpechko et al.* [2010] and *Barnes et al.* [2016].

2.2. SAM and ENSO Indices

The SAM is defined as the first empirical orthogonal function (EOF) of monthly mean zonal mean zonal wind anomalies at each pressure level between 20° and 80°S during 1970 to 2004. The SAM time series is defined as the standardized first principal component, with a positive annular mode index in the troposphere defined as a strengthening and poleward shift of the midlatitude jet relative to climatology. For the CESM-LE, the first EOF is defined at each pressure level using data from all 42 members; each member's annular mode time series is then calculated by projecting its zonal mean zonal wind anomalies at each time step onto the EOF derived from the full ensemble. The SAM indices for CMIP5 are calculated in a similar manner—the first EOF is defined at each level using data from all available simulations for each model, so that each model's EOF and annular mode time series are calculated separately. The MERRA reanalysis SAM index time series is calculated using monthly mean data from 1979 to 2004. Most of this analysis is focused on November-December-January (NDJ), as these are the months of greatest response to volcanic forcing.

The ENSO phase is determined using the Niño 3.4 index. Following *Lehner et al.* [2016], the monthly sea surface temperature anomalies are averaged over the Niño 3.4 region (170°–120°W, 5°S–5°N), detrended using a quadratic fit and then standardized. Our results are not sensitive to the use of Niño 3 (5°S–5°N, 150–90°W) or Niño 4 (5°S–5°N, 160°E–150°W) indices in place of Niño 3.4. The ENSO index is determined separately for each member of the CESM-LE and for each simulation in CMIP5. The ENSO phase is then classified according to the value of the detrended, standardized Niño 3.4 index. A positive ENSO (i.e., El Niño) event is defined when this value exceeds 0.5, and a negative ENSO (i.e., La Niña) event is defined when this value is less than −0.5; all other years are defined as neutral ENSO.

In addition to evaluating the SAM response to volcanoes, we also examine the eddy-driven jet response, as the midlatitude jet is a dominant feature of the midlatitude circulation and is directly related to the storm tracks. While the midlatitude jet and the SAM responses are related, calculating the jet response allows for independent analysis of changes in jet position and jet speed [e.g., *Thomas et al.*, 2015]. We use 10 m zonal mean zonal winds to assess the changes in jet position and strength. Additionally, changes in the 10 m winds can be linked to changes in surface wind stress, which is important for determining the ocean response to volcanic forcing. This methodology is discussed in detail in the supporting information.

3. Results

3.1. Southern Hemisphere Circulation Response to Volcanoes

Figure 1 displays the NDJ CESM-LE and CESM-Pacemaker zonal mean zonal wind anomalies following the Pinatubo eruption. Figures 1a and 1b highlight contrasting patterns simulated by two members of the CESM-LE; simulation 14 shows a strongly positive SAM (Figure 1a), while simulation 32 shows a strongly negative SAM (Figure 1b), highlighting the contribution of internal variability in any one realization. The ensemble mean of CESM-LE (Figure 1c), indicative of the forced response to Pinatubo, shows a forced positive SAM response, with positive zonal wind anomalies at 60°S and negative zonal wind anomalies at 40°S. This response is robust and significant, with over 70% of the simulations agreeing on the sign of the SAM response (Figure 1d).

The Northern Hemisphere also demonstrates large internal variability, with a positive annular mode response evident in simulation 14 and a negative response evident in simulation 32 (Figures 1a and 1b). Unlike the SAM, the forced NAM response is not significant (Figure 1d). *Barnes et al.* [2016] find that the CMIP5 Northern Hemisphere circulation anomalies following Pinatubo do not project well onto the zonal mean NAM but do exhibit robust poleward shifts of the midlatitude jet when separated into North Pacific and North Atlantic sectors. We focus on the Southern Hemisphere for the remainder of this study.

The forced (e.g., ensemble mean) response in the CESM-Pacemaker runs (Figure 1e) is similar to that of the CESM-LE, showing a positive SAM, albeit one with weaker magnitude. The CESM-Pacemaker ensemble mean also shows positive zonal wind anomalies in the subtropics and tropics that are not present in the CESM-LE. The differences between the forced responses in the CESM-Pacemaker and CESM-LE ensembles are highlighted in Figure 1f. The hemispheric symmetry of the anomalies in Figure 1f are indicative of the circulation response to ENSO, emphasizing that ENSO may play a role in the differences between the CESM-Pacemaker and CESM-LE responses (see discussion in section 3.3).

The results shown in Figure 1 indicate that the simulated forced response to Pinatubo is a robust positive SAM but that large internal variability exists. We explore this further by plotting histograms of the NDJ SAM

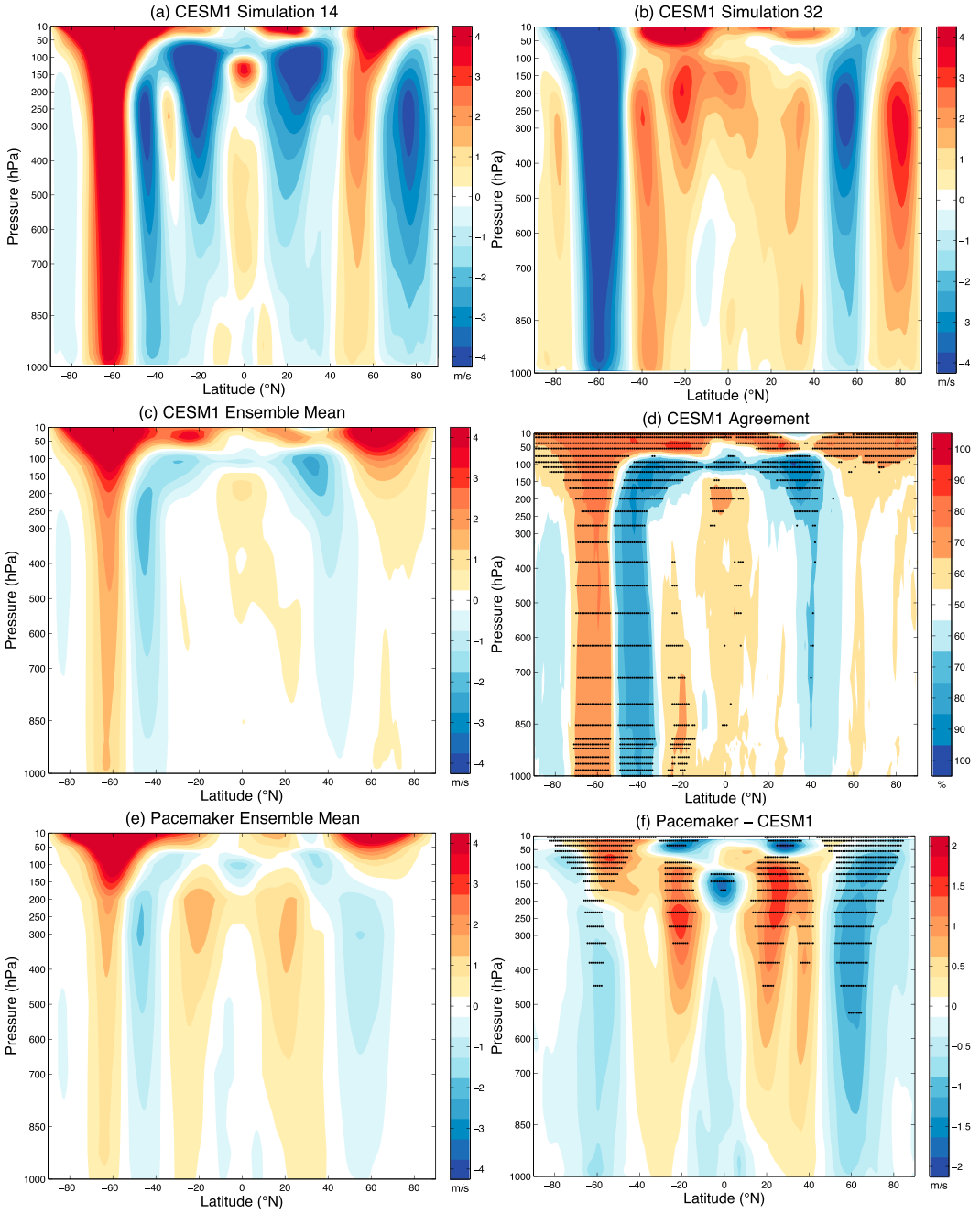

Figure 1. Zonal mean zonal wind anomalies in NDJ after Pinatubo from the CESM-LE for (a) simulation 14, (b) simulation 32, and (c) the ensemble mean of all 42 simulations. (d) Agreement in sign of the zonal wind anomalies following Pinatubo across the 42 simulations. (e) As in Figure 1c but for the ensemble mean of the 10 CESM-Pacemaker simulations. (f) Figure 1e minus Figure 1c. In Figure 1d, stippling indicates agreement on the sign of the anomaly at 95% confidence using a binomial distribution. In Figure 1f, stippling indicates significance at 95% confidence according to a difference of means test.

index in years with and without volcanoes for the CESM-LE and CESM-Pacemaker simulations (Figure 2). The NDJ SAM index is calculated for all years from 1970 to 2004; the red lines show the SAM indices in the years following the eruptions of Pinatubo and El Chichón (1991–1992 and 1982–1983), while the blue lines show the SAM indices in all other years. In the CESM-LE (solid lines), the post-volcano SAM distribution is more positive than the SAM distribution in years without volcanoes. The two SAM distributions are significantly different from each other at 95% confidence according to the two-sample Kolmogorov-Smirnov test (K-S test).

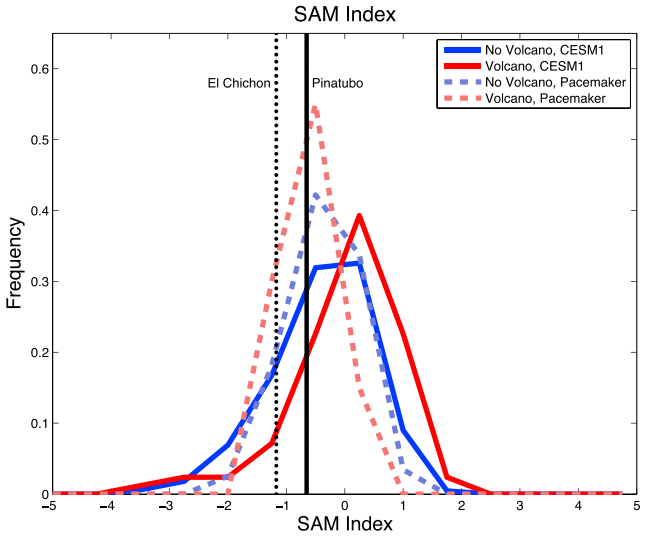

Figure 2. The distribution of NDJ 700 hPa SAM indices for years without volcanoes (blue lines) and years with volcanoes (red lines) for the CESM-LE simulations (solid lines) and the CESM-Pacemaker simulations (dashed lines). The observed mean NDJ SAM indices following El Chichòn and Pinatubo are shown in the dashed and solid black vertical lines, respectively.

The CESM-Pacemaker simulations (dashed lines) differ much less, and the difference is not significant, hinting at the impacts of ENSO variability on the SAM response. Analagous figures based on jet position and strength present a complementary picture of the circulation response, showing a poleward shift and strengthening of the surface zonal winds in response to volcanic forcing (see supporting information).

The observed NDJ SAM indices following Pinatubo and El Chichón (black lines) are both negative but well within the range of variability found in the CESM-LE and CESM-Pacemaker simulations. Thus, the observed SAM responses to the Pinatubo and El Chichón eruptions are not at odds with the modeled forced response to these eruptions, since internal variability can overwhelm the forced response.

3.2. Comparison With CMIP5

An advantage of using the CESM-LE is that all simulations use the same model, thus isolating internal variability from model structural uncertainty. However, to demonstrate that the forced SAM signal is robust across a range of models and not just a feature of CESM1, we perform similar analysis on 155 simulations from 37 CMIP5 models. Figure 3 shows the evolution of the SAM index for the 24 months following the two volcanic eruptions in the CESM-LE (Figure 3a) and CMIP5 (Figure 3b). In both figures, the evolution of the mean SAM index across all simulations (black line) is compared to the observed SAM anomalies following Pinatubo (solid red line) and El Chichón (dashed red line). Both the CESM-LE and the CMIP5 models show a positive SAM response in the 2–7 months following an eruption; in many months, the sign of the response is significant at 95% confidence (black dots). In both CMIP5 and the CESM-LE, internal variability (gray shading) is larger than the forced SAM anomalies. The CESM-Pacemaker ensemble mean (light blue line

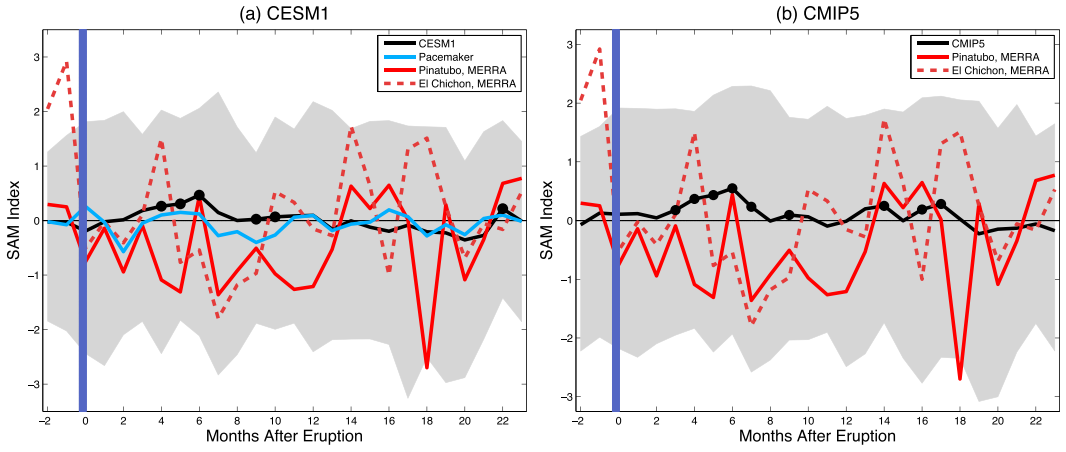

Figure 3. Evolution of monthly 700 hPa SAM indices over the 24 months following a volcanic eruption (month zero) for (a) the CESM-LE and (b) the CMIP5 models. The black curves show the ensemble mean values, with black dots indicating months in which the sign of the response is positive and significant at 95% confidence. The light blue curve in Figure 3a denotes the CESM-Pacemaker ensemble mean. The red lines indicate the observed SAM indices following Pinatubo (solid) and El Chichón (dashed). The gray shading indicates the 95th percentile range of SAM indices across all model runs.

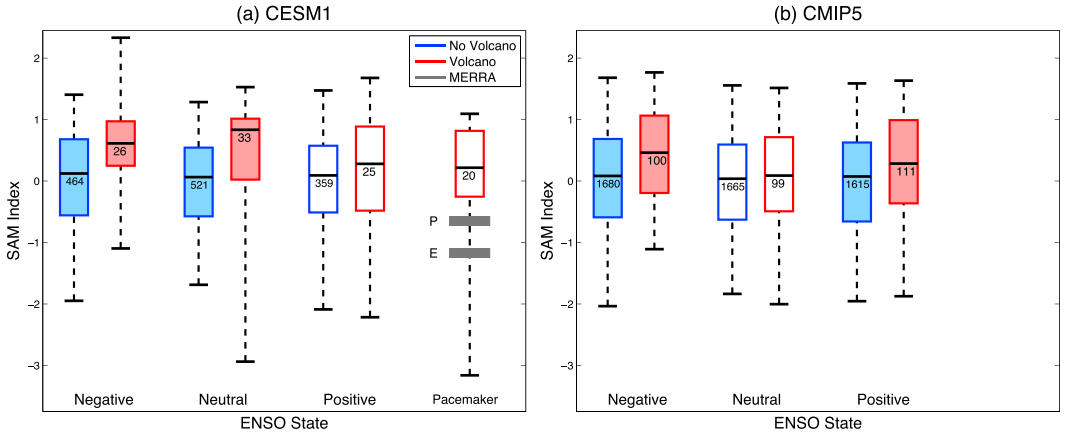

Figure 4. Mean NDJ SAM index as a function of ENSO state for (a) CESM-LE and CESM-Pacemaker simulations and (b) CMIP5. Years following volcanoes are in red, while all other years are in blue. Shaded boxes indicate that the median value of the SAM index in years with volcanoes is significantly different from that in years without volcanoes at 95% confidence. The numbers inside the boxes list the number of simulations in each ENSO state. The whiskers show the 95th percentile range across the simulations. The horizontal gray boxes in Figure 4a indicate the observed values of the NDJ SAM index after El Chichòn (E) and Pinatubo (P) based on MERRA reanalysis.

in Figure 3a) lacks the magnitude and robustness of the positive SAM response in the CESM-LE, with SAM indices near zero following the eruption. This is likely due to the positive ENSO state of the CESM-Pacemaker runs (as will be discussed in the next section). Finally, the observed SAM indices following Pinatubo (solid red) and El Chichón (dashed red) differ from the forced responses in the CESM-LE and CMIP5 ensembles, and from each other, but they largely fall inside the 95th percentile of the SAM responses for both model ensembles (gray shading), once more highlighting the dominance of internal climate variability.

3.3. Impact of ENSO State

Both Pinatubo and El Chichón occurred during positive ENSO events [see *Lehner et al.*, 2016, Figure 1]. While some research indicates that an El Niño might actually be more likely in the 1 to 2 years following a large eruption [e.g., *Adams et al.*, 2003; *Emile-Geay et al.*, 2008; *Stevenson et al.*, 2016], the positive ENSO events after El Chichón and Pinatubo were already underway before the eruptions occurred. Therefore, questions regarding this causality are set aside for the purposes of this study, and we focus our analysis on the year immediately following the eruption. We emphasize that while previous studies [e.g., *Karpechko et al.*, 2010; *Barnes et al.*, 2016] have hinted at a relationship between ENSO state and the SAM response to volcanic forcing, we use a larger sample of model simulations (52 CESM1 and 155 CMIP5 composited over two eruptions—over 200 simulations in total) for a robust assessment of any connections between ENSO state and the SAM phase.

Figure 4 shows the NDJ SAM indices in 1982–1983 and 1991–1992 (red boxes) and all other years (blue boxes) as a function of ENSO state for both the CESM-LE (Figure 4a) and CMIP5 (Figure 4b). Regardless of ENSO state, years following major tropical volcanic eruptions show a more positive median SAM index (black lines) than years without major tropical eruptions in both CMIP5 and the CESM-LE. In the CESM-LE, this positive SAM response is much stronger (and significant at 95% confidence) in simulations with negative or neutral ENSO states compared to simulations with positive ENSO states (including the CESM-Pacemaker runs), which show a much smaller and insignificant increase in the SAM index. The CMIP5 SAM responses are similar to the CESM-LE responses during positive and negative ENSO states; however, the CMIP5 response during neutral ENSO is weaker than that of the CESM-LE. Note that when all 207 simulations are analyzed together (i.e., combining CMIP5 and the CESM-LE), the SAM is significantly more positive in years with major tropical eruptions than in years without, regardless of ENSO state (see supporting information Figure S3). These results are consistent with Figures 2 and 3 and demonstrate that the forced response to tropical eruptions is a positive SAM.

Going further, we find that the SAM index following eruptions in simulations with a negative ENSO state is significantly larger than the SAM index in simulations with a positive ENSO state (compare red boxes in Figure 4). This difference is significant at 95% confidence for the CESM-LE and CMIP5 combined analysis and at 90% confidence for the CESM-LE and CMIP5 individually. Thus, while years following eruptions all exhibit more positive NDJ SAM indices when compared to all other years, this positive SAM anomaly is largest during negative

ENSO conditions. One might expect that this difference is due to a simple offset of the circulation response to volcanic eruptions by the response to ENSO [e.g., *L'Heureux and Thompson*, 2006]. However, if this were the case, one would expect that the SAM responses for positive and negative ENSO states would be different even in years without volcanoes, but this is not evident (compare blue boxes in Figure 4). Thus, the reasons for the differences between the SAM anomalies during positive and negative ENSO states are likely more complicated than a simple offset due to the ENSO response. Recent results by *Welhouse et al.* [2016] emphasize the different mechanisms of the SAM-ENSO teleconnection in summer versus winter, further highlighting the complexities of the SAM-ENSO relationship.

The observed SAM indices (horizontal gray boxes in Figure 4a) following both the El Chichón and Pinatubo eruptions fall below the median model SAM indices, but within the internal variability exhibited for neutral and positive ENSO states in the CESM-LE and CMIP5 (Figure 4). It is worth noting that the observed SAM anomaly after El Chichón is just outside the natural variability of the response for simulations with negative ENSOs in both CMIP5 and the CESM-LE, while the observed SAM anomaly following Pinatubo is just inside this range. This suggests that the observed SAM anomaly following El Chichón may have been unlikely in a year with a negative ENSO event. Finally, the CESM-Pacemaker simulations (Figure 4a) show a weaker SAM response to volcanic forcing compared to the CESM-LE simulations (see also Figure 1f)—a weaker response that is likely due, at least in part, to the positive ENSO states of all 20 CESM-Pacemaker simulations.

4. Conclusions

The Southern Hemisphere circulation response to volcanic forcing is a robust positive Southern Annular Mode (SAM) in both the CESM1 Large Ensemble and the CMIP5 models. However, due to the large internal variability, this forced response may be obscured in any individual simulation. At least some of this internal variability can likely be attributed to the state of ENSO: negative ENSO states exhibit a stronger SAM anomaly, while positive ENSO states exhibit a weaker SAM anomaly following eruptions. Internal variability coupled with the positive ENSO states observed after both El Chichón and Pinatubo places the observations into context. We argue that the models and observations are not in opposition—the observed SAM indices fall well within the distribution of modeled SAM indices, especially when accounting for ENSO state. Ultimately, while the volcanoes examined here do produce a forced tropospheric circulation response in the Southern Hemisphere, this response does not appear strong enough to overwhelm other sources of internal climate variability.

Acknowledgments

We thank Tingting Fan and Adam Phillips at the National Center for Atmospheric Research (NCAR) for conducting and providing us with the Pacemaker simulations and assisting us in obtaining the CESM1 Large Ensemble Data and Haibo Liu and the Lamont-Doherty Earth Observatory for obtaining the CMIP5 data. We also thank Flavio Lehner for helpful discussions and feedback and the two anonymous reviewers for their comments and suggestions. The MERRA data used in this study have been provided publicly by the Global Modeling and Assimilation Office (GMAO) at NASA Goddard Space Flight Center through the NASA GES DISC online archive (http://disc.sci.gsfc.nasa.gov/daac-bin/DataHoldings.pl). M.C.M. and E.A.B. were supported, in part, by the Climate and Large-scale Dynamics Program of the National Science Foundation under grant 1419818. NCAR is sponsored by the National Science Foundation.

References

Adams, J. B., M. E. Mann, and C. M Ammann (2003), Proxy evidence for an El Niño-like response to volcanic forcing, *Nature*, *426*, 274–278, doi:10.1038/nature02101.

Barnes, E. A., L. M. Polvani, and S. Solomon (2016), Robust wind and precipitation responses to the Mount Pinatubo eruption, as simulated in the CMIP5 models, *J. Clim.*, *29*, 4763–4778, doi:10.1175/JCLI-D-15-0658.1.

Christiansen, B. (2008), Volcanic eruptions, large-scale modes in the Northern Hemisphere, and the El Nino-Southern Oscillation, *J. Clim.*, *21*, 910–922.

Driscoll, S., A. Bozzo, L. Gray, A Robock, and G. Stenchikov (2012), Coupled Model Intercomparison Project 5 (CMIP5) simulations of climate following volcanic eruptions, *J. Geophys. Res.*, *117*, D17105, doi:10.1029/2012JD017607.

Emile-Geay, J., R. Seager, M. A. Cane, E. R. Cook, and G. H. Haug (2008), Volcanoes and ENSO over the past millennium, *J. Clim.*, *21*, 3134–3148, doi:10.1175/2007JCLI1884.1.

Graf, H., I. Kirchner, A. Robock, and I. Schult (1993), Pinatubo eruption winter climate effects: Model versus observation, *Clim. Dyn.*, *9*, 81–93.

Hitchman, M. H., M. McKay, and C. R. Trepte (1994), A climatology of stratospheric aerosol, *J. Geophys. Res.*, *99*, 20,689–20,700.

Karpechko, A., N. P. Gillett, M. Dall'Amico, and L. J. Gray (2010), Southern Hemisphere atmospheric circulation response to the El Chichón and Pinatubo eruptions in coupled climate models, *Q. J. R. Meteorol. Soc.*, *136*, 1813–1822.

Kay, J. E., et al. (2015), The Community Earth System Model (CESM) large ensemble project: A community resource for studying climate change in the presence of internal climate variability, *Bull. Am. Meteorol. Soc.*, *96*, 1333–1349, doi:10.1175/BAMS-D-13-00255.1.

Kosaka, Y., and S.-P. Xie (2013), Recent global-warming hiatus tied to equatorial Pacific surface cooling, *Nature*, *501*, 403–407, doi:10.1038/nature12534.

Lehner, F., A. P. Schurer, G. C. Hegerl, C. Deser, and T. L. Frölicher (2016), The importance of ENSO phase during volcanic eruptions for detection and attribution, *Geophys. Res. Lett.*, *43*, 2851–2858, doi:10.1002/2016GL067935.

L'Heureux, M., and D. W. J. Thompson (2006), Observed relationships between the El Niño-Southern Oscillation and the extratropical zonal-mean circulation, *J. Clim.*, *19*, 276–287.

Ottera, O. H. (2008), Simulating the effects of the 1991 Mount Pinatubo volcanic eruption using the Arpege atmospheric general circulation model, *Adv. Atmos. Sci.*, *25*, 213–226, doi:10.1007/s00376-008-0213-3.

Perlwitz, J., and H.-F. Graf (1995), The statistical connection between tropospheric and stratospheric circulation of the Northern Hemisphere in winter, *J. Clim.*, *8*, 2281–2295.

Rienecker, M. M., et al. (2011), MERRA: NASA's Modern-Era Retrospective Analysis for Research and Applications, *J. Clim.*, *24*, 3624–3648.

Robock, A. (2000), Volcanic eruptions and climate, *Rev. Geophys.*, *28*, 191–219.

Robock, A., and J. Mao (1995), The volcanic signal in surface temperature observations, *J. Clim.*, *8*, 1086–1103.

Robock, A., T. Adams, M. Moore, L. Oman, and G. Stenchikov (2007), Southern Hemisphere atmosphere, *Geophys. Res. Lett.*, *34*, L23710, doi:10.1029/2007GL031403.

Roscoe, H., and J. Haigh (2007), Influences of ozone depletion, the solar cycle and the QBO on the Southern Annular Mode, *Q. J. R. Meteorol. Soc.*, *133*, 1855–1864.

Rozanov, E. V., M. E. Schlesinger, N. H. Andronova, F. Yang, S. L. Malyshev, V. A. Zubov, T. A. Egorova, and B. Li (2002), Climate/chemistry effects of the Pinatubo volcanic eruption simulated by the UIUC stratosphere/troposphere GCM with interactive photochemistry, *J. Geophys. Res.*, *107*, 4049, doi:10.1029/2001JD000974.

Santer, B. D., et al. (2013), Human and natural influences on the changing thermal structure of the atmosphere, *Proc. Natl. Acad. Sci. U.S.A.*, *110*, 17,235–17,240, doi:10.1073/pnas.1305332110.

Solomon, S. (1999), Stratospheric ozone depletion: A review of concepts and history, *Rev. Geophys.*, *37*, 275–316, doi:10.1029/1999RG900008.

Stenchikov, G., K. Hamilton, A. Robock, V. Ramaswamy, and M. D. Schwarzkopf (2002), Arctic Oscillation response to the 1991 Pinatubo eruption: Effects of volcanic aerosols and ozone depletion, *J. Geophys. Res.*, *107*, 4803, doi:10.1029/2002JD002090.

Stenchikov, G., K. Hamilton, R. J. Stouffer, A. Robock, V. Ramaswamy, B. Santer, and H.-F. Graf (2006), Arctic Oscillation response to volcanic eruptions in the IPCC AR4 climate models, *J. Geophys. Res.*, *111*, D07107, doi:10.1029/2005JD006286.

Stevenson, S., B. Otto-Bliesner, J. Fasullo, and E. Brady (2016), "El Niño like" hydroclimate responses to the Last Millennium volcanic eruptions, *J. Clim.*, *29*, 2907–2921, doi:10.1175/JCLI-D-15-0239.1.

Taylor, K. E., R. J. Stouffer, and G. A. Meehl (2012), An overview of CMIP5 and the experiment design, *Bull. Am. Meteorol. Soc.*, *93*, 485–498.

Thomas, J. L., D. W. Waugh, and A. Gnanadesikan (2015), Southern Hemisphere extratropical circulation: Recent trends and natural variability, *Geophys. Res. Lett.*, *42*, 5508–5515, doi:10.1002/2015GL064521.

Trepte, C. R., R. E. Veiga, and M. P. McCormick (1993), The poleward dispersal of Mount Pinatubo volcanic aerosol, *J. Geophys. Res.*, *98*, 18,563–18,573, doi:10.1029/93JD01362.

Welhouse, L. J., M. A. Lazzara, L. M. Keller, G. J. Tripoli, and M. H. Hitchman (2016), Composite analysis of the effects of ENSO events on Antarctica, *J. Clim.*, *29*, 1797–1808, doi:10.1175/JCLI-D-15-0108.1.